Supplementary Information for

Identifying General Reaction Conditions for Mechanoradical Natural Hydrogen Production

Wuge Cui[1], Yunfeng Liang[1], Yoshihiro Masuda[1], Takehiro Hirose[2], Takeshi Tsuji[1]**

[1] *Department of Systems Innovation, The University of Tokyo; Tokyo, 113-8656, Japan.*

[2] *Kochi Institute for Core Sample Research, Japan Agency for Marine-Earth Science and Technology; Nankoku, Kochi 783-8502, Japan.*

Corresponding Author

E-mail: liang@sys.t.u-tokyo.ac.jp (Y.L.)

E-mail: tsuji@sys.t.u-tokyo.ac.jp (T.T.)

Supplementary information includes:

Materials and Methods

Figs. S1 to S7

Movie 1: $SiOH_2$ generation (First step of hydrogen generation)

This movie shows the reaction process by introducing charge transfer and the main product is $SiOH_2$, which is an intermediate product of hydrogen. The movie is designed to show the surface reaction on the upper surface only, there are similar chemical reactions on the lower surface (not shown).

Movie 2: H_2 generation (Second step of hydrogen generation)

This movie shows the reaction process by introducing inverse charge transfer and H_2 is generated rapidly. The movie is designed to show the surface reaction on the upper surface only, there are similar chemical reactions on the lower surface (not shown).

Movie 3: O_2 generation (Oxygen generation process)

This movie shows that one oxygen molecule is generated on an oxygen-rich surface with SiOO as an intermediate product. The movie is zoomed in to show the oxygen molecule generation clearly. A full scale of the system is shown in Figure S7.

Materials and Methods

Fig. S1 shows the systems that we have employed initially. We first incorporated spin polarization due to the presence of the active radical surface of the quartz, but no hydrogen was produced. Then, we tried to include impurities, such as iron atoms, replacing silicon atoms on the surface of quartz at various locations, and iron in an aqueous solution. We anticipated a more rapid hydrogen production under the influence of iron, but there is no hydrogen generated, and three potential reasons for the absence of production in the simulations can be identified. Firstly, charge transfer was not implemented in the simulation, based on our successful experiences, it is crucial to guarantee a robust positive charge on the surface-active silicon atoms. Secondly, the system surface may not be fully reductive, with some active oxygen atoms exposed on the surface potentially capturing free hydrogen atoms. Thirdly, the simulation time for hydrogen is limited due to computational constraints. Not only do we require additional simulations involving more systems, but experimental validation is also needed. Given the increased complexity introduced by the presence of iron, this article will primarily concentrate on modelling hydrogen generation, temporarily setting aside the discussion of iron's effects. Further simulations and experiments are expected to comprehensively explore these aspects.

The different surfaces of the reducing environment when the quartz cleavage is shown in Fig. S2. They were used in the simulation to try to produce hydrogen. The use of charge transfer and inverse charge transfer on the reducing surfaces can lead to successful hydrogen production. To achieve a localized oxygen-free environment requires that there are no exposed oxygen atoms on the ruptured surface. On the (100) Q3 surface and the (100) Q2 surfaces, we analyzed the amount of hydrogen produced concerning different temperatures and pressures. Based on the ordering of surface reconstruction energy[1], the (001) surface is the easiest to form, while the (100)

surface falls in the middle. In hydrolyzed surface (101) is the most abundant. However, the possibility of forming a surface without reactive oxygen exposure is also low for the (001) surface, particularly when Si is in a Q2 configuration. Consequently, we opted to focus our primary discussion on hydrogen generation on the Q3 surface of (100). Simultaneously, hydrogen generation simulations on the Q2 surface of (001) were also conducted, and the results are detailed in the supporting materials.

The potential energy for generating hydrogen and not generating hydrogen is shown in Fig. S3. The potential energy of the hydrogen-producing case is lower than that of the non-hydrogen-producing case for all the different pressure and temperature conditions modelled. This means that the production of hydrogen is reasonable in these cases.

In Fig. S4, it is evident that, while the system's pressure fluctuates within a certain range, the overall mean values exhibit minimal changes. The mean values are summarized in Table 1. Notably, the pressure within the Ice VII system is significantly higher compared to the water system.

Simulations illustrating hydrogen generation through charge transfer on a distinct surface are shown in Figs S5 and S6. To validate the charge transfer in generating hydrogen on a different surface, we designed this simulation. Importantly, it is crucial to emphasize that this remains a reducing surface without reactive oxygen exposure, ensuring the successful generation of hydrogen. We consistently observed the formation of $SiOH_2$ after the introduction of charge transfer, followed by the generation of SiOH and H_2 upon inverse charge transfer.

In the oxygen-generating system (Fig. S7), we employed a cleaved surface designed to hide reactive oxygen atoms and another surface designed to enrich reactive oxygen atoms. This aimed to facilitate hydrogen generation on the Si-terminated surface without a charge transfer. However,

despite these efforts, the absence of charge transfer resulted in the generation of SiH rather than hydrogen, while oxygen was successfully produced on the oxygen-enriched surface. To minimize interference between the two layers, we put the entire system within a $1.97 \times 9.40 \times 1.09$ nm^3 box. Additionally, 1.15 nm water films were introduced on two distinct surfaces, allowing ample space on both sides. This configuration was implemented to avoid proton transfer through the Grotthuss mechanism[2,3].

References

1. V. V. Murashov, Reconstruction of pristine and hydrolyzed quartz surfaces. *J. Phys. Chem. B* **109**, 4144–4151 (2005).
2. W. A. Adeagbo, N. L. Doltsinis, K. Klevakina, J. Renner, Transport processes at α-quartz-water interfaces: insights from first-principles molecular dynamics simulations. *ChemPhysChem* **9**, 994–1002 (2008).
3. M. Ledyastuti, Y. Liang, T. Matsuoka, The first-principles molecular dynamics study of quartz-water interface. *Int. J. Quantum Chem.* **113**, 401–412 (2013).

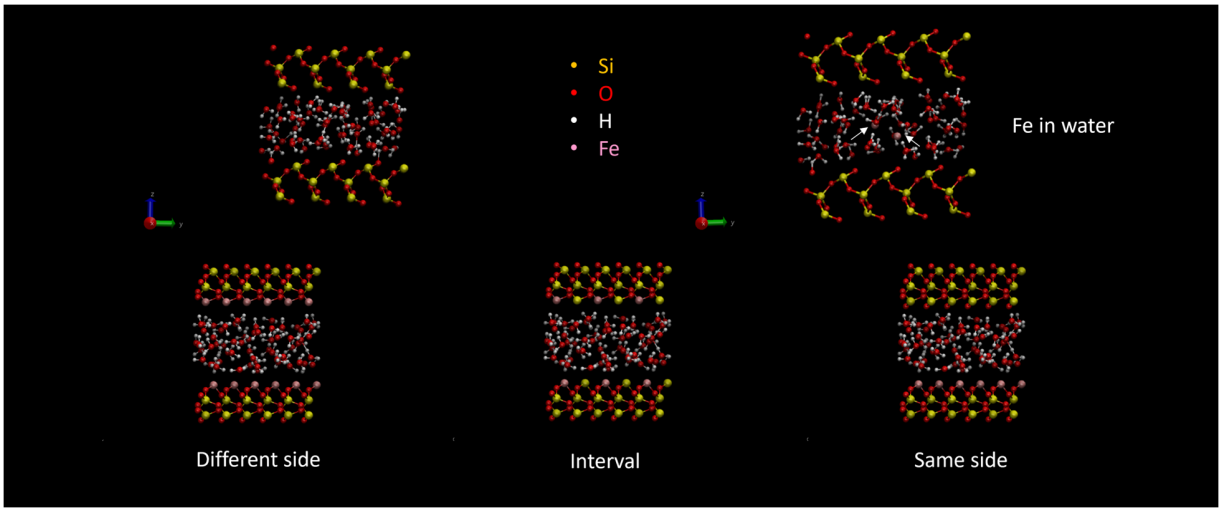

Figure S1. In the absence of charge transfer, our attempts to introduce iron into various systems for hydrogen production have been conducted. Each system's simulation time is from 0.3 ps to 0.4 ps, and temperatures is from 500 K to 1,500 K.

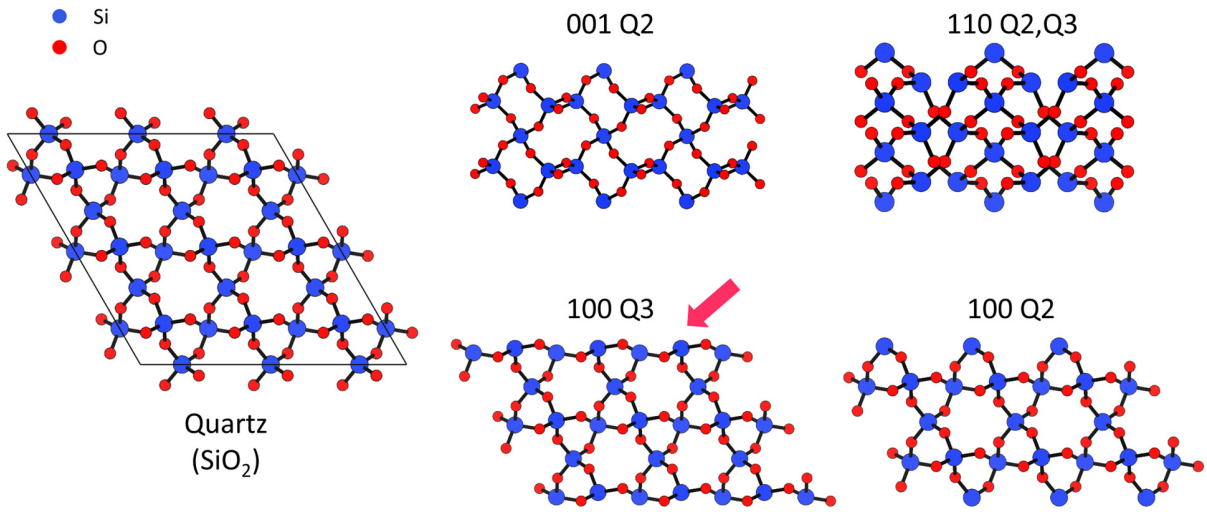

Figure S2. Various surfaces result from quartz cleavage. The labels 001, 110, and 100 represent the Miller index of the quartz. Q2 indicates silicon bonded with two other atoms, while Q3 indicates silicon bonded with three atoms.

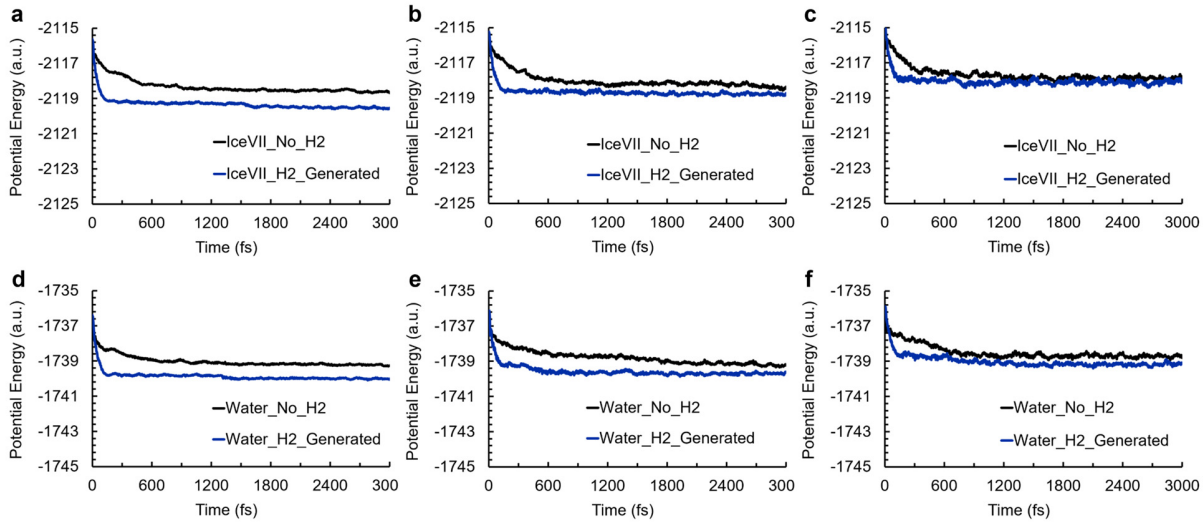

Figure S3. Potential energy of hydrogen generated, and no hydrogen generated system. a, 500 K Ice VII, **b**, 1,000 K Ice VII, **c**, 1,500 K Ice VII, **d**, 500 K water, **e**, 1,000 K water, **f**, 1,500 K water.

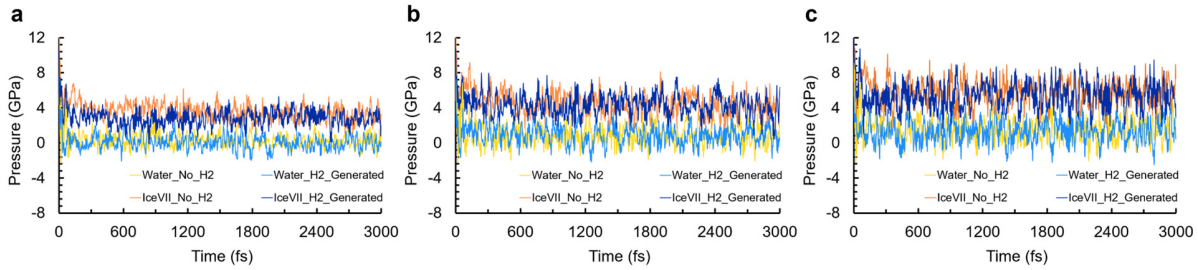

Figure S4. Variation of system pressure with time at different temperatures. a, 500 K, **b**, 1,000 K, **c**, 1,500 K.

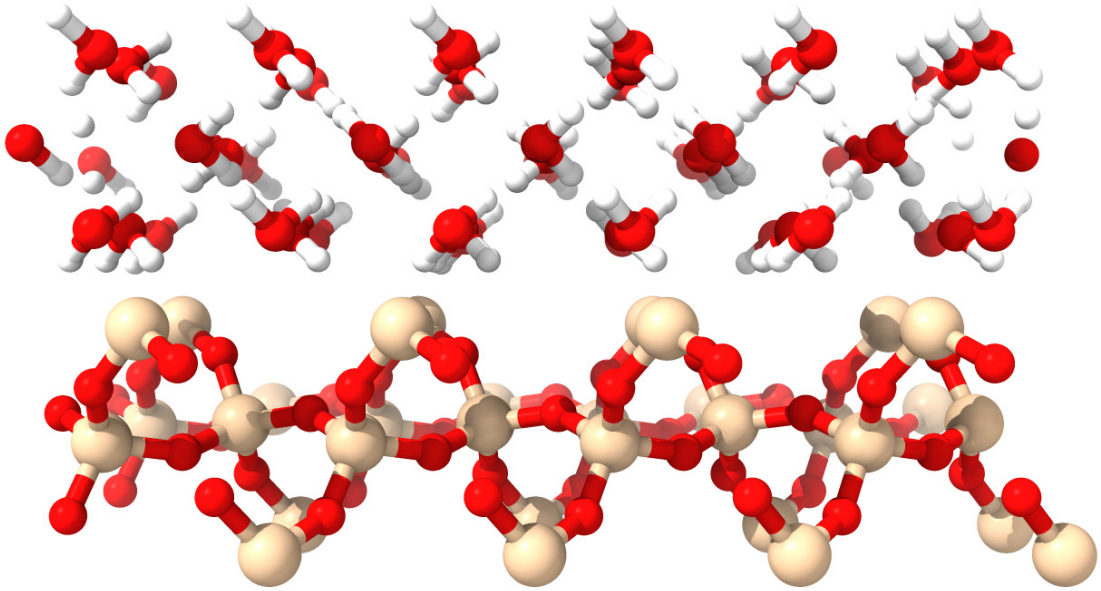

Figure S5. Si-terminated Q2 model. Hydrogen was generated on different surfaces of quartz, and reactive oxygen atoms are also hidden within these surfaces.

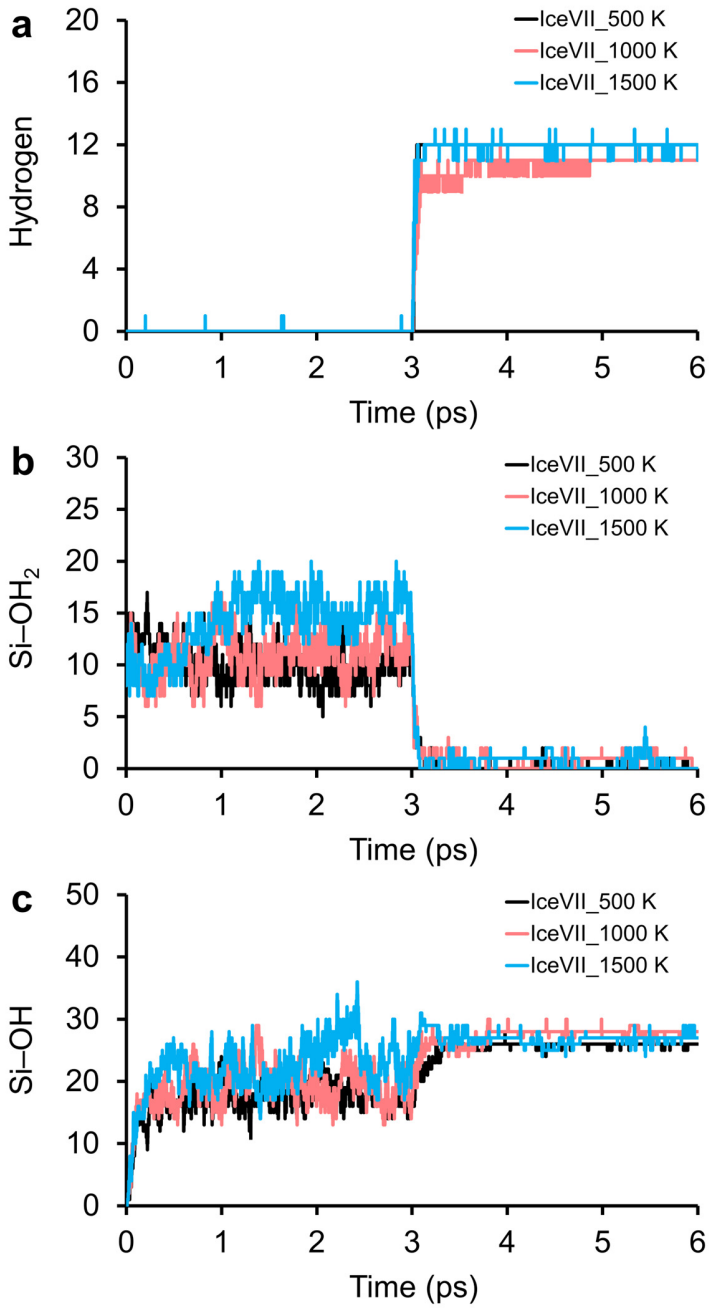

Figure S6. The amount of hydrogen, $SiOH_2$, and SiOH produced at the quartz Q2 fracture surface and ice VII at different temperatures exhibits variation over simulation time. a, hydrogen production with charge transfer and inverse charge transfer. **b**, Amount of $SiOH_2$ with charge transfer and inverse charge transfer. **c**, Amount of SiOH with charge transfer and inverse charge transfer.

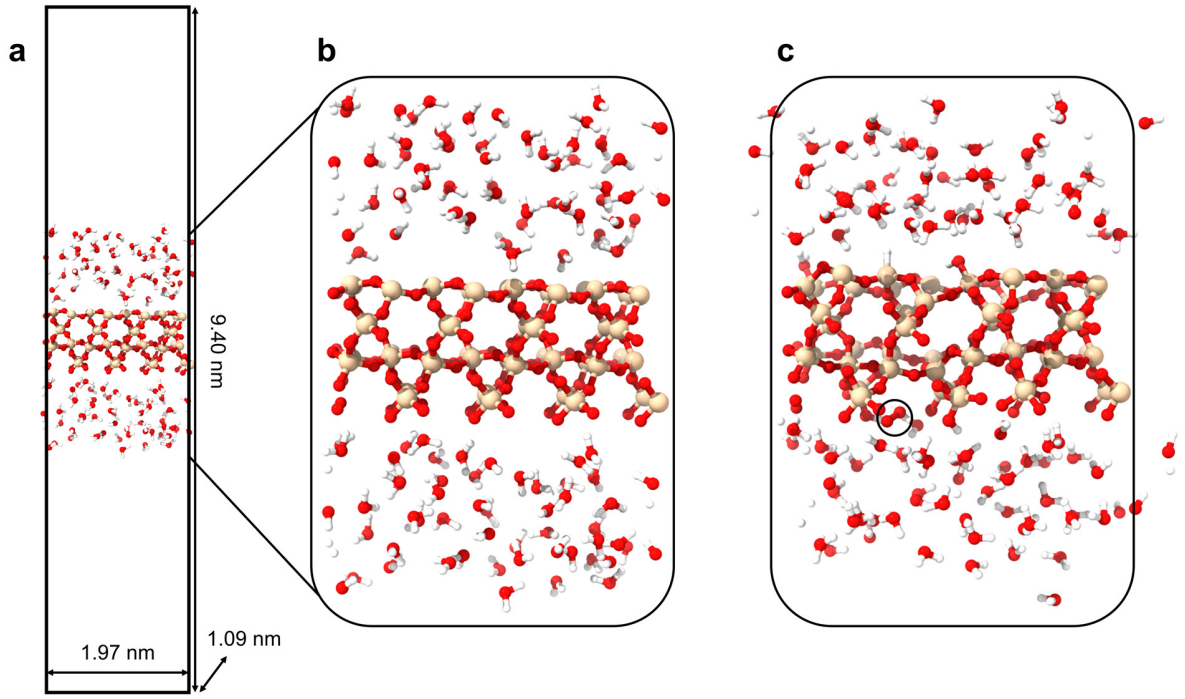

Figure S7. Simulation system of oxygen generation. a, snapshot of the simulation box, **b**, snapshot of the initial state, **c**, snapshot of the oxygen generation state.